

Multi-Stage Fusion Architecture for Small-Drone Localization and Identification Using Passive RF and EO Imagery: A Case Study

Thakshila Wimalajeewaewelwala*, Thomas W. Tedesso and Tony Davis
Air and Missile Defense Sector (AMDS)
Johns Hopkins University Applied Physics Laboratory (JHU/APL)
11100 Johns Hopkins Rd, Laurel, MD 20723
*Thakshila.Wimalajeewa@ieee.org

Abstract—Reliable detection, localization and identification of small drones is essential to promote safe, secure and privacy-respecting operation of Unmanned-Aerial Systems (UAS), or simply, drones. This is an increasingly challenging problem with only single modality sensing, especially, to detect and identify small drones. In this work, a multi-stage fusion architecture using passive radio frequency (RF) and electro-optic (EO) imagery data is developed to leverage the synergies of the modalities to improve the overall tracking and classification capabilities. For detection with EO-imagery, supervised deep learning based techniques as well as unsupervised foreground/background separation techniques are explored to cope with challenging environments. Using real collected data for Group 1 and 2 drones, the capability of each algorithm is quantified. In order to compensate for any performance gaps in detection with only EO imagery as well as to provide a unique device identifier for the drones, passive RF is integrated with EO imagery whenever available. In particular, drone detections in the image plane are combined with passive RF location estimates via detection-to-detection association after 3D to 2D transformation. Final tracking is performed on the composite detections in the 2D image plane. Each track centroid is given a unique identification obtained via RF fingerprinting. The proposed fusion architecture is tested and the tracking and performance is quantified over the range to illustrate the effectiveness of the proposed approaches using simultaneously collected passive RF and EO data at the Air Force Research Laboratory (AFRL) through ESCAPE-21 (Experiments, Scenarios, Concept of Operations, and Prototype Engineering) data collect.

livery, rescue operations, wireless communication, and sheer enjoyment of flight, the threat of small UASs (sUASs) to national security is increasing [1], [2], [3]. Based on the payload capability, the drones can be used for various illegal activities and even be used as dangerous weapons after loading them with explosive material [4], [5]. In order to implement an effective counter-UAS (cUAS) system to prevent any security breaches or undesirable impact on the public safety and national security, it is vital to detect and identify these small, in particular Group 1 and 2 [6], drones reliably and understand their intent. There are a variety of sensing modalities that can be used for drone surveillance including radar, electro-optical (EO), infrared (IR) imagery, passive radio frequency (RF), acoustic, etc.. Recent review papers present the advantages and disadvantages of the individual modalities for drone detection and identification [7], [8].

As shown in multiple studies, the ability of reliable detection, classification and localization of drones with only a single modality is quite challenging. The conventional radar (S and X band) suffers from small radar cross section (RCS) of most of these small drones, thus, the detection and discrimination capability is limited. To obtain higher range resolution, radar at higher frequencies (Ku/K/Ka/millimeter wave bands) could be used; however, the maximum range that the drones can be detected/classified is very limited. For example, the authors in [9] quantified the classification accuracy with micro-doppler imagery of a Ku band radar where the maximum distance considered is $\sim 100m$. Video or imagery is another commonly used modality to detect and track drones; however, the performance depends on the drone size, availability of line of sight (LOS), and resemblance of other objects like birds. Drone detection and classification using Deep Learning with EO imagery is an active research area, however, for small drones (Group 1, 2), reliable detection is still challenging even with the recent advances in deep learning when the drones occupy only a few pixels in the image pixel plane. On the other hand foreground/background separation algorithms to detect drones can perform poor in the presence of high clutter and slowly moving clouds, and also when the drones hover for a long time. Most of the commercial drones designed for surveillance and hobbyists use downlink transmission to relay messages to a remote controller. These downlink signals can be used for detection, classification and localization of drones when available. Further, passive RF (passive RF and P-RF, for passive RF, are used interchangeably in the rest of the paper) can be used to infer useful information regarding the drone intent by analyzing the transmit waveform patterns and the RF fingerprint [10], [11], [12]. Acoustic is another modality that can convey information regarding the drone payload via acoustic fingerprinting [13]. However, research

TABLE OF CONTENTS

1. INTRODUCTION.....	1
2. PROBLEM FORMULATION/SOLUTION OVERVIEW	3
3. PERFORMANCE ANALYSIS	5
4. DISCUSSION	9
5. CONCLUSIONS.....	9
6. APPENDIX	9
ACKNOWLEDGMENTS	10
REFERENCES	10
BIOGRAPHY	11

1. INTRODUCTION

While unmanned aerial systems (UASs) or more specifically, drones, are being actively used for a variety of civil and commercial applications including photography, package de-

DISTRIBUTION STATEMENT A: Approved for public release: distribution is unlimited
979-8-3503-0462-6/24/\$31.00 ©2024 IEEE

arXiv:2406.16875v1 [eess.SP] 30 Mar 2024

				
Aircraft	Inspired Flight (USA)	DJI	DJI	DJI
Model	IF 1200	Matrice 600	Phantom 4 Pro V2	Mavic Air 2
Type	VTOL	VTOL	VTOL	VTOL
Use	Payload Carrier, Red Target	Red Target	Red Target	Red Target
Weight kg(lbs.)	13.4(29.5)	9.2(20.3)	1.4(3)	0.6(1.3)
Telemetry Radio	Microhard pMDDL2450	DJI proprietary	DJI proprietary	DJI proprietary
Telemetry SW	Mavlink	Lightbridge	Ocusync	Ocusync 2

Figure 1: AFRL ESCAPE2021 data collect: Types of drones used as targets; picture credit: AFRL/RI [13]

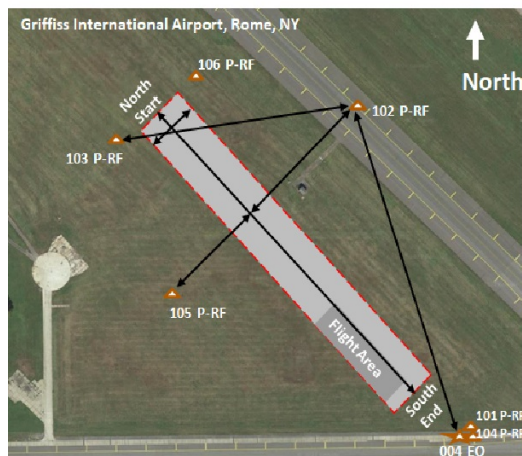


Figure 2: AFRL ESCAPE2021 data collect: Sensor Layout with passive RF and EO Sensors; picture credit: AFRL/RI [13]

on understanding the full capabilities of acoustic modality for drone detection and identification is still in its infancy.

The goal of this paper is to evaluate the drawbacks of individual passive RF and EO modalities using collected data for Group 1, 2 drones and exploit the diversity across multiple modalities to design a reliable fusion architecture for drone detection, identification and tracking. In this work, we consider how passive RF can be integrated with EO to boost the overall detection and identification performance of small drones. To detect the drones in the 2D image plane with EO, supervised deep learning algorithms as well as advanced foreground/background separation algorithms are investigated. We show that the state-of-the-art deep learning techniques fail to reliably detect and identify drones when the drones are far away (several hundreds of meters) from the camera and occupy only few pixels in the image plane. When the drones appear to be point targets in the image plane, advanced foreground/background separation techniques can be more reliable in detecting drones (as moving outliers in the image) than deep learning techniques. In order to label the detected drones at the 'point target' stage in 2D image-

plane, we incorporate device ID obtained via RF fingerprinting using passive RF when available. RF fingerprinting is quite challenging for drones when they transmit similar waveforms; however, the anomalous behavior of the RF front-end of the drone transmitter provides a unique RF fingerprint for each drone which can be learned using advanced deep learning techniques. To map the EO detections with passive RF, we use time-difference-of-arrival (TDOA) based localization with passive RF in the sensor plane and project the 3D location estimates to the 2D image plane for detection-to-detection association. Finally, a Kalman filter is used on the composite EO and RF detections in the 2D image plane to form tracks for each detected drone along with the device labels.

Description of Data and Drones

In order to benchmark the detection and classification capabilities of the proposed architecture, we use simultaneously collected real passive RF and EO data for four small drones. This data is collected at the 2021 ESCAPE II Data Collection (termed as ESCAPE2021 in the rest of the paper) hosted by AFRL at the Griffiss International Airport, Rome, NY (GIA-RME) and the AFRL Stockbridge, NY Test Site (STS) [14]. Multi-modal data is collected for multiple target types (ground vehicles, drones and dismounts) with a variety of sensor types including radar, passive RF, EO, IR, seismic, and acoustic sensors over different days. In this work, we use data for drone targets collected at EO and passive RF sensors where a target description is shown in Fig. 1 and the sensor layout is illustrated in Fig. 2. The drone targets include 3 DJI drones and one Inspired Flight (IF) 1200 as shown in Fig. 1. Phantom and Mavic can be considered to belong to Group 1, while m600 and IF1200 can fall into the Group 2 category.

More information about this dataset is provided in Section 3. Using this data, the goal is to quantify (i) the range from the camera that the small drones can be reliably detected using the deep learning algorithms as well as advanced foreground/background separation algorithms using EO imagery, (ii) device ID accuracy of the four drones with AI-enabled RF fingerprinting, and (iii) the tracking performance of the RF and EO fusion architecture over the range from the EO camera.

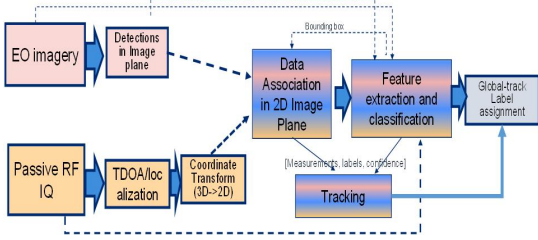


Figure 3: EO and Passive RF individual operations and the fusion architecture for detection, identification and tracking of drones

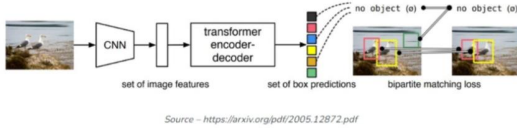


Figure 4: DETR concept for image detection [20]

2. PROBLEM FORMULATION/SOLUTION OVERVIEW

The proposed fusion architecture is depicted in Fig. 3 along with individual operations of each modality.

Drone Detection with EO Imagery

To detect drones in EO imagery, we explore both state-of-the-art deep learning based techniques as well as foreground/background separation techniques and illustrate the advantages of one over the other.

Image Detection with Deep Learning—There is an abundant of research in the recent past to detect objects in EO-IR imagery using deep learning techniques such as YOLO versions [15], [16], fast-Region-based Convolutional Neural Network (fast-RCNN) [17], Detection Transformer (DETR), etc...[18], [19], [20]. As stated in the Introduction section, most of the deep learning techniques struggle to detect small drones when they are far away from the camera and occupy only a small number of pixels in the image. Further, fine classification (e.g., multiple DJI drones) is also challenging except getting a generic identifier such as 'drone'. Among the existing deep learning based image detectors, DETR [21] is shown to have a good accuracy and run-time performance trade-off over other existing deep learning models against the challenging Common Objects in Context (COCO) object detection dataset. Thus, we use DETR as the deep learning based image detector in this work.

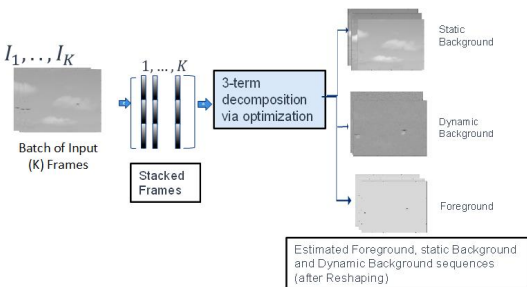


Figure 5: Overview of RPCA for foreground/background separation with EO imagery

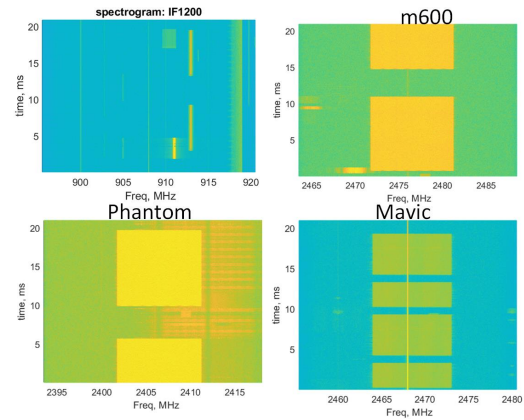


Figure 6: Spectrogram of the 4 drones (from left to right; IF1200, m600, Phantom, Mavic), Center frequencies of IF1200, m600, Phantom and Mavic are 908MHz, 2476MHz, 2406MHz and 2468MHz, respectively

DETR is a set-based object detector using a Transformer on top of a convolutional backbone (Fig. 4). It uses a conventional CNN backbone to learn a 2D representation of an input image. The model flattens it and supplements it with a positional encoding before passing it into a transformer encoder [21]. The DETR model is loaded from hugging-face.co, an online resource for sharing open-source models. Our DETR model was trained using pytorch lightning, a machine learning (ML) framework built on top of pytorch optimized for multi-graphics processing unit (GPU) training. This allowed us to train models and iterate faster. Our training data is a drone object detection dataset from [22]. This allowed us to train and iterate the model much faster than native pytorch, and improve the performance using various built-in tools to aid training such as learning rate schedulers and stochastic weight averaging [23]. The augmentations used were horizontal flip (50% of samples), color jitter (25%), random brightness/contrast (20%) and motion blur (10%).

Image Detection via Foreground/Background Separation—There is a long history for detecting moving objects in imagery using foreground/background separation techniques [24], [25]. Robust Principal Component Analysis (RPCA) is a subspace method which is shown to perform better than other comparable techniques for foreground detection with complex dynamic backgrounds [26], [27], [28]. While RPCA is quite extensively investigated for image detection in video surveillance applications, there is no sufficient study in the literature to understand its capabilities in detecting drones, especially, when the drones are far away from the camera (in the region where most of the state-of-the-art deep learning techniques fail) and when the background is highly dynamic due to clouds, occlusions and the impact of other moving objects. In this work, we explore RPCA for drone detection with EO imagery. In general, RPCA operates in batch mode where a collection of frames is processed at a time. Let I_1, \dots, I_K denote a set of K -frames captured by a camera with frame dimension $N_1 \times N_2$. By stacking all the columns of a given frame in to a vector, a matrix $X \in R^{N \times K}$ is created where the k -th column of X corresponds to the vectorized version of I_k (Fig. 5) and $N = N_1 N_2$. In the RPCA framework, the matrix X is decomposed to a low-rank (background) matrix, a sparse (foreground) matrix and a dense error (dynamic background) matrix so that

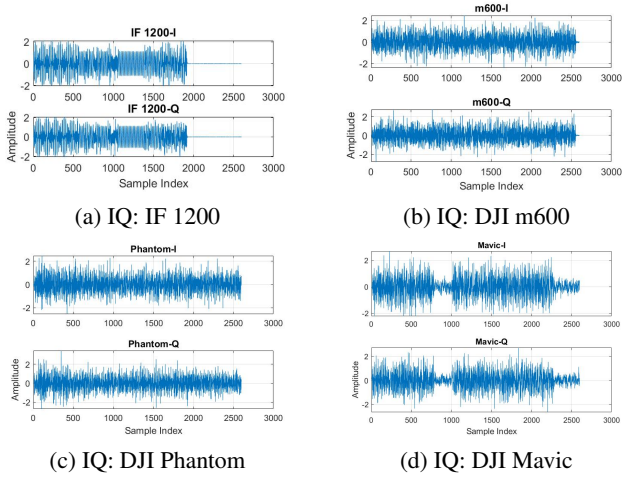


Figure 7: Baseband IQ representation of the downlink waveforms of 4 drones

$$X = L + S + E$$

where $L, S, E \in R^{N \times K}$ represent the low-rank, sparse and error matrix, respectively. The three matrices L, S, E are recovered by solving the following optimization problem:

$$\begin{aligned} \min_{L, S, E} & \|L\|_* + \tau \|S\|_1 + \lambda \|E\|_F^2 \\ \text{such that } & X = L + S + E \end{aligned} \quad (1)$$

where $\|\cdot\|_*$, $\|\cdot\|_1$ and $\|\cdot\|_F$ denote the nuclear norm, l_1 norm and the Frobenius norm of a matrix, respectively, and τ and λ are penalty parameters. Finding the global optimal solution of (1) in closed-form is a difficult problem, and alternating-direction-method of multiplier (ADMM) is a widely used approach which solves (1) iteratively by optimizing one variable keeping the rest constant [27] (See Appendix). The ADMM based foreground/background separation algorithmic steps are summarized in Algorithm 1.

Algorithm 1 Foreground/Background Separation via ADMM

Inputs; X , scaler parameters λ, τ, ρ
 Initialization: $Y, S, E, \beta > 0$,

While not converged **do**

$$\begin{aligned} UWV^T &= \text{svd}\left(X - E^k - S^k + \frac{Y^k}{\beta^k}\right) \\ L^{k+1} &= U \Pi_{\frac{1}{\beta}}(W) V^T \\ S^{k+1} &= \Pi_{\frac{\tau}{\beta^k}}\left(X - E^k + \frac{Y^k}{\beta^k} - L^{k+1}\right) \\ E^{k+1} &= (1 + 2\lambda/\beta^k)^{-1}(X - L^{k+1} - S^{k+1} + Y^k/\beta^k) \\ Y^{k+1} &= Y^k + \beta^k(X - L^{k+1} - S^{k+1} - E^{k+1}) \end{aligned}$$

$$\beta^{k+1} = \rho \beta^k$$

End

$\Pi_{\alpha}(x) = \text{sign}(x) \cdot \max\{|x| - \alpha, 0\}$
 svd : singular value decomposition

Outputs: $\hat{S}, \hat{L}, \hat{E}$

While RPCA is a promising approach for foreground and background separation, its computational complexity is quite significant (due to the need of singular value decomposition) compared to other basic techniques for foreground/background separation when the image frame dimension is large. In order to implement RPCA in real-time, we run RPCA after partitioning the original images where individual partitions can be processed in parallel. After processing each batch with parallel partitions, the individual partitions are mapped back to the original image dimension, so that RPCA can be implemented in near real time.

Drone Detection, Localization and Identification with Passive RF

Most drones (unless they full autonomous) use a down-link communication protocol to relay messages to a remote controller. While drones may not transmit continuously depending on the intent of the drone, the purpose is to leverage the useful information inferred from passive RF whenever available to support the tracking and identification capabilities with only EO data. As shown in Fig. 1, the 4 drones considered in this work use proprietary waveforms for downlink communication.

Drone Identification via RF Fingerprinting—In Fig. 6, the spectrogram is shown for the 4 drones considered. It is noted that DJI m600 and Phantom share very similar timing and frequency characteristics, while DJI Mavic and IF 1200 are quite different from the first two. Nevertheless, we train a deep learning model to classify these 4 drones extracting the RF fingerprint from the baseband IQ-level data. The deep learning model operates with raw IQ data and pre-processing as discussed below is done to extract IQ vectors for training/test.

Localization—With multiple passive RF sensors, we explore a TDOA-based approach for drone localization. In order to get 3D position estimates of the drones, at least 4 passive receivers are necessary.

Passive RF Data pre-Processing for RF Fingerprinting and Localization—The data is captured at 25MHz centered at center frequencies listed in Fig. 6 for each drone. It is noted that the data link used by DJI drones are pretty wideband while the waveform used by IF 1200 has a hop pattern within the 25MHz bandwidth. The next step is to identify the center frequency of the hop (mainly for the IF1200, since for DJI drones, it is fixed), and extract a baseband IQ vector of 250kHz wide by low pass filtering and downsampling the data at Nyquist rate. The reason for selecting a relatively small frequency band for RF fingerprinting is to get a relatively a moderate size IQ vector over a reasonable time interval to capture rising and falling edges of the transmitted waveforms. By observing the packet length of all four drones, the decision making time for RF fingerprinting is taken as 0.0210s which corresponds to 5250 samples at 250kHz sampling rate. After edge detection of the extracted IQ vector, the noise component is removed so that the effective length of IQ is set to 2600. The pre-processed waveforms used for training/test are shown in Fig. 7.

For TDOA computation using passive RF IQ, the original data is down converted to 10MHz and perform noise filtering to extract only the desired signal component at every 0.0210s . TDOAs are estimated by computing the cross correlation of each sensor pair considered.

Table 1: Scenarios and Targets used to Train Deep Learning Model for RF Fingerprinting

Scenario	Target	Devices	passes
r15	IF 1200	101, 102, 103	01, 02
r15	m600	104, 105, 106	01, 02
r13	Mavic	101, 102, 103	01, 02
r13	Phantom	104, 105, 106	01, 02

Detection-Detection Association and Tracking with EO and Passive RF in 2D

Let (X, Y, Z) be the world coordinates of the target with respect to the camera position and (x, y) be the corresponding location in the image pixel plane. Then, (x, y) can be expressed as

$$w \times [x \ y \ 1] = [X \ Y \ Z \ 1] \times [R; T] \times K \quad (2)$$

where K is the camera intrinsic matrix, R is the camera rotation matrix, T is a translation vector, w is a scaler. In ESCAPE 2021 data collect, the camera intrinsic matrix parameters are recorded and calibration is done to estimate the other extrinsic parameters (R and T).

The estimated target locations with respect to the EO sensor are projected onto the 2D image plane using (2). Then, the passive RF detections and EO detection are ordered in time in the 2D image plane and, a 2D Kalman filter with a constant velocity model is used for 2D tracking.

3. PERFORMANCE ANALYSIS

This section provides an overview of the experiments and overall performance of individual modalities as well as with the fusion architecture. Experimentation consist of multiple steps; (i) train a deep learning model to obtain drone fingerprint using passive RF IQ data, (ii) TDOA estimation and localization with passive RF IQ (iii). 2D detections via RPCA and DETR with EO imagery (iv) End-to-End architecture testing.

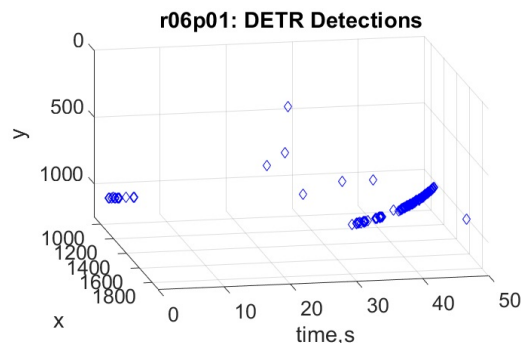
To train the deep learning classifier for RF fingerprinting, we consider the scenarios listed in Table 1. It is noted that, we follow a similar scenario and device labeling as in [14] just for simplicity.

Each collect per target has multiple passes to impose redundancy which is useful mainly in deep learning exercises. Each scenario is 50s long, which provides ~ 2300 IQ examples on average with 0.0210s decision making time for RF fingerprinting (some scenarios can be longer than this). We consider different devices and different passes to ensure diversity across communication channels. With the scenario selection as in Table 1, each target has ~ 11,000 labeled IQ vectors for training.

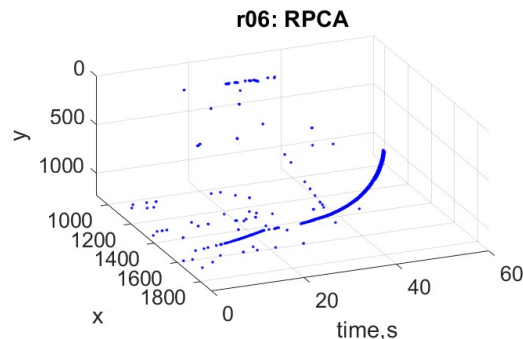
To test the end-to-end architecture for detection localization and tracking, three scenarios are considered as depicted in Table 2. In scenario 1 (r06p01), only DJI Phantom flies from North to South. In Scenario 2 (r14p01), DJI Mavic and DJI Phantom drones fly at a constant altitude over ~ 500m while in Scenario 2 (r16p01), IF 1200 and m600 are flying along the same path as in r14p01.

Table 2: Scenario and Target Description used to Test End-to-End EO-RF Fusion Architecture

Scenario	Targets	Flight path	Distance
r06p01	Phantom	North to South	~ 500m
r14p01	Phantom, Mavic	North to South	~ 500m
r16p01	m-600, IF 1200	North to South	~ 500m



(a) r06; DETR 2D Detections



(b) r06; RPCA 2D Detections

Figure 8: r06, Estimated foreground mask over time (range) with different algorithms

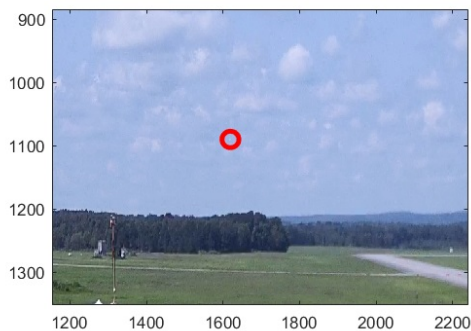


Figure 9: First Detect of Phantom in r04 with RPCA; range 435m from EO004 camera.

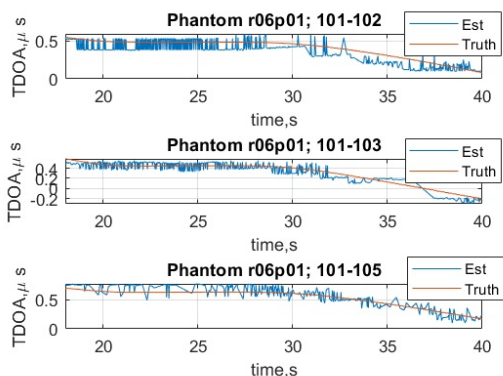


Figure 10: r06; TDOA estimates with sensor pairs d101-d102, d101-d103, d101-d105; Time is with respect to the start time of the EO camera E001 recording; for r06, there is a time lag between EO and passive RF recordings

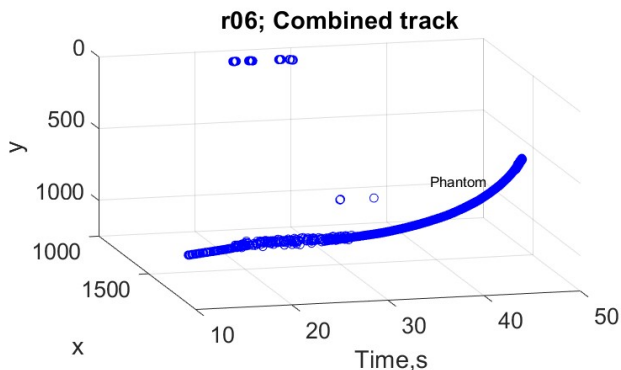


Figure 11: r06; Combined track with associating passive RF projections with 2D Image detections

Analyzing r06

r06: Drone Detection Performance with EO Imagery—In Scenario r06, Phantom starts flying from north at a distance of $\sim 500m$ from the EO sensor which is located at south. Fig. 8 illustrates the RPCA and DETR detections over 2D image plane over time (and range). The EO data is sampled at $30Hz$ and has a frame size of 3840×2160 (full frame is not shown in the figure for clarity). It is noted that detections with r06 EO imagery is quite challenging due to the slow moving clouds. Fig. 9 shows the original image when the RPCA first detects the target where the drone is $435m$ away from the camera. Note that RPCA parameters are optimized to obtain reliable detections over the entire trajectory, so some clutter detections (especially coming from the clouds) are visible towards the beginning of the trajectory, which go away with Kalman Filtering as shown later in this section. DETR struggles to get reliable detections until the drone is about $200m$ away from the camera.

r06: Drone Classification Performance with RF Fingerprinting—Classification performance of Phantom using the trained model to classify 4 drones using passive RF IQ similar to the scenario discussed under next scenario (Analyzing r14), thus, is avoided here for brevity.

r06: TDOA Based 3D Localization—In r06 where a single drone is flying, all six passive RF receivers are tuned to the

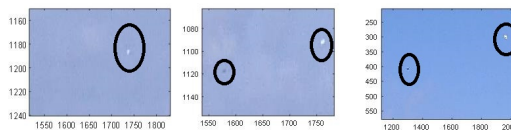


Figure 12: r14: DJI Mavic (negative contrast) and DJI Phantom (Positive contrast) in the same image frame; different range from the EO camera location; (Left) at $\sim 450m$, (middle) $\sim 300m$, (right) at $\sim 200m$. It is noted that, Mavic is not captured at all in the image plane at range $\sim 450m$.

same downlink frequency of the drone, $2.406GHz$. For 3D localization, the sensors 101, 102, 103, and 105 are used. With 3 independent pairs of TDOA, spherical intersection algorithm [29] is used to find the 3D drone position. Fig. 10 illustrates the TDOA estimates for r06 (compared to the ground truth compared with actual distances) while Fig. 11 illustrates the combined track in the 2D plane. It is noted that some of discontinuities observed in EO only detection is compensated for after integrating passive RF and the true track is given a unique ID. It is worth noting that, since passive RF has a time lag compared to the EO recording in this scenario, early part of the trajectory is still missed.

Analyzing r14

In r14, Mavic and Phantom drones fly simultaneously starting at a range of $\sim 500m$ away from the EO sensor.

r14: Drone Detection Performance with EO Imagery—It is noted that Mavic and Phantom drones are light weight (Fig. 1) and very small which are very hard to detect when they are far away from the camera. Zoomed images at different ranges from the camera are shown in Fig. 12 to depict the point-target nature of Mavic and Phantom at various ranges.

As seen in Fig. 12, the two drones have positive and negative contrast with respect to the background image, thus it is hard to optimize the image detection algorithms to detect both simultaneously. For RPCA, we consider this observation as a side information and optimize the algorithm to detect objects with positive contrast and the object with negative contrast in parallel and fuse them together. For RPCA, we used 30 frames at once for batch processing (i.e. $1s$ of latency with $30Hz$ frame rate). Fig. 13 shows the estimated foreground mask (binary value indicating the centroid of the bounding box) over time (range) for scenario r14p01.

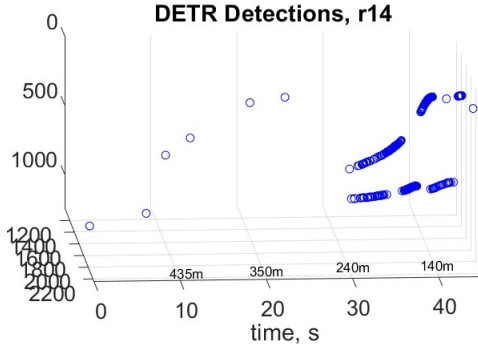
From Fig. 13, it is observed that the DETR algorithm fails to detect the drones until they are about $240m$ away from the camera. The RPCA algorithm on the other hand, can detect both drones much earlier (Mavic at $\sim 350m$ with negative contrast and Phantom at $\sim 440m$ with positive contrast). Note that what is shown in Fig. 13 are raw detections in the image plane, and some of the isolated false alarms could be eliminated once the tracker is run. This is done with the composite detections after integrating with passive RF below; however, in order to get EO-only tracks, a 2D Kalman filter can run on the raw EO detections.

r14: Drone Classification Performance with RF Fingerprinting

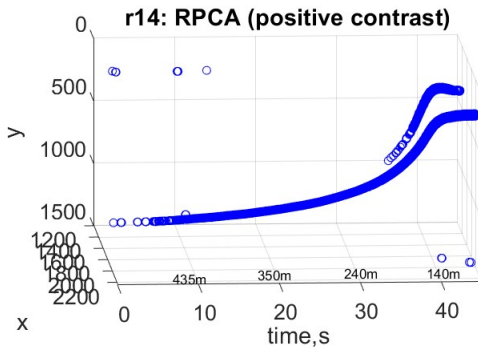
This section discusses the device ID capability of passive RF for scenario r14. The developed deep learning model consists of a set of convolutional, pooling and dilation layers and the architecture and parameters are summarized in Fig. 14.

Table 3: Average Confidence of the Trained Deep Learning Model for RF Fingerprinting when Tested with Mavic and Phantom in r14p01

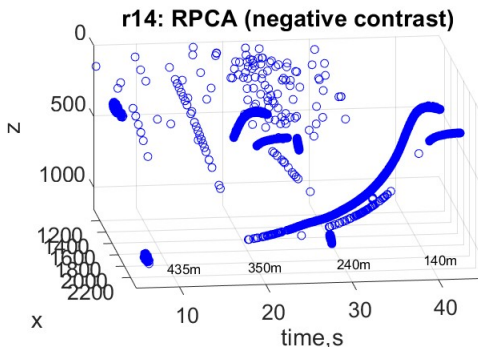
Tested Class	Avg Conf on IF 1200	Avg Conf on Mavic	Avg Conf on Phantom	Avg Conf on m600
Mavic	0.002	0.988	0.011	0
Phantom	0.007	0.004	0.995	0.001



(a) DETR, both Mavic and Phantom are reliably detected around $\sim 240m$ away from the camera



(b) RPCA, positive contrast, Phantom is detected at $\sim 440m$, while Mavic is not detected early



(c) RPCA, negative contrast, Mavic is first detected at $\sim 350m$, while Phantom is not detected early

Figure 13: r14, Estimated foreground mask over time (range) with different 2D image detection algorithms

Layer	# of Filters (nodes)	Kernel size	Stride size	Dilation rate	Activation	Shape
Input						(2600, 1,2)
Conv1D	128	(11,1)	(1,1)	1	Relu	(2600,1,128)
MaxPooling	-	(3,1)	(2,1)	-		(1299,1,128)
Conv1D	256	(7,1)	(1,1)	2	Relu	(1299,1,256)
MaxPooling	-	(3,1)	(2,1)	-		(649,1,256)
Conv1D	384	(5,1)	(1,1)	4	Relu	(649,1,384)
MaxPooling	-	(3,1)	(2,1)	-		(324,1,384)
Conv1D	256	(3,1)	(1,1)	8	Relu	(324,1,396)
Conv1D	128	(3,1)	(1,1)	-	Relu	(324,1,128)
MaxPooling	-	(3,1)	(2,1)	8		(161,1,128)
Flatten	-					20608
Dense	1024	-	-	-	Relu	1024
Dense	512	-	-	-	Relu	512
Dense	512	-	-	-	Relu	512
Output					Softmax	4

Figure 14: Configuration of the developed Deep Learning model for RF fingerprinting

As discussed in Section 2, the designed deep learning based classifier is trained with all 4 drone classes in this ESCAPE data collect using the scenarios listed in Table 1. It is noted that the training data is constructed using $r13$ and $r15$ where $r13$ contains the same targets as in $r14$ while $r15$ contains the same targets as in $r16$. However, in $r13$ and $r15$, drones fly south to north while in $r14$ and $r16$, the drones fly north to south. For the test phase, we consider the scenarios $r14$ and $r16$.

In the test phase, the trained model gives a confidence value between $[0, 1]$ for each trained class that the model believes the test vector belongs. The average confidence for each trained class (over all the time indices) in the trajectory when tested with Mavic and Phantom is summarized in Table 3. It is worth noting that the output layer of the trained model gives a confidence value which can be thresholded (or take the maximum over all trained classes) to declare the corresponding drone class. It can be seen that while few examples of Mavic get confused with Phantom, overall, the trained model provides a promising confidence for the true class.

r14: Final Tracker in the 2D Plane with Passive RF and EO Fusion

As observed in Fig. 13, while RPCA based EO detections perform much better than DETR, it still struggles to detect Mavic at early stages in $r14$. Also, RPCA does not do any classification, but only detection. To incorporate the device ID obtained via RF fingerprinting and compensate for the poor performance at the far range in detection with only EO, we performed TDOA based localization until the drones are about $300m$ away from the EO camera (i.e. about $30s$ after drones start flying). In Scenario $r14$, only 3 passive RF receivers are tuned to one drone, thus the number

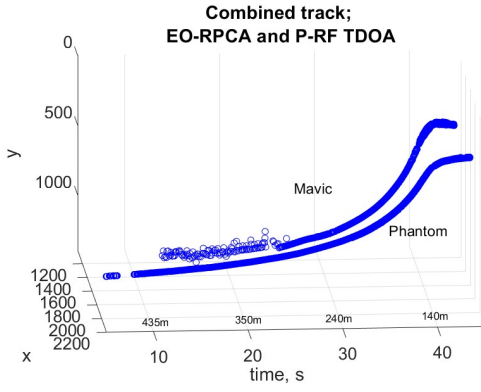


Figure 15: r14: Final track with EO and P-RF fusion, passive RF location estimates are used until the EO only forms a consistent track for each drone, device ID is associated via RF fingerprinting

of sensors is not sufficient to perform 3D localization with spherical intersection. It is noted that the drones are flown at a constant altitude in this data collect, thus, using that as a side information, three passive RF receivers are used to estimate the other two dimensions of the targets in the sensor plane via maximum likelihood estimation. After TDOAs are estimated using passive RF IQ (by computing the cross correlation among sensors), the locations are found using the maximum likelihood approach. Let $\Delta\tau_i$ be the TDOA of the i -th sensor pair. Then, the location of the target with respect to a reference point is estimated as

$$\hat{r}_t = \underset{r_t}{\operatorname{argmin}} \left\{ \sum_{i=1}^L \left(\frac{\|r_t - r_{i,1}\|_2 - \|r_t - r_{i,2}\|_2}{c} - \Delta\tau_i \right)^2 \right\}$$

where L is the number of sensor pairs, c is the speed of light, $r_t = [X_t, Y_t, Z_t]$ is the location of the target and the $r_{i,1}$ is the location of the 1st sensor in the i -th sensor pair, with respect to a reference point.

For Mavic, the passive RF sensors d101-d103 are used while for Phantom devices d104-d106 are used.

It is worth noting that the P-RF sensor recordings have a lag ($\sim 12s$) compared to the EO recordings, thus passive RF detections are shifted by $12s$ to be synchronised with EO detections. Also, for the devices d104-d106, there is a time offset about $6s$ between d106 and the other two which was appropriately shifted. It is further worth noting that, in ESCAPE 2021 data collect, only three passive RF sensors are monitoring any given drone when two drones are flying simultaneously. Ideally, at least 4 sensors are needed to do 3D geolocation using TDOA. However, using the fact that the all drones in ESCAPE 2021 data collect fly at approximately a constant altitude, we used three passive RF receivers to do 3D localization using the altitude as a side information (with some uncertainty). Taking all these factors into account, and after performing detection-detection association in the 2D image plane, the final composite tracks for r14 are obtained as shown in Fig. 15. Regarding track labeling, until passive RF is integrated, the EO detections are associated via the Hungarian algorithm [30] to associate detections over frames which provides a notional track ID for multiple tracks. Once passive RF is integrated and associated with EO detections, the corresponding track labels are replaced by the passive RF device labels obtained via fingerprinting. In case where there

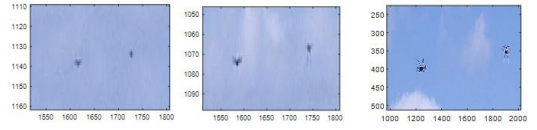


Figure 16: r16: m-600 and IF1200 in the same image frame; different ranges from the EO camera location, (left) $\sim 450m$, (middle) $\sim 300m$, (right) $\sim 200m$

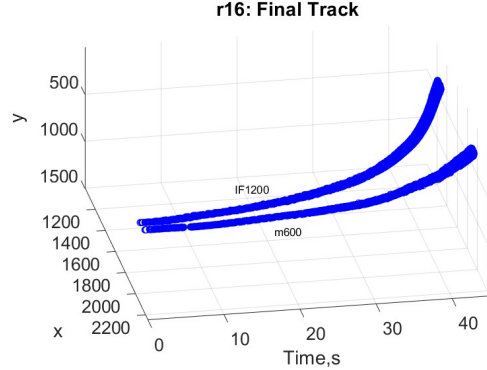


Figure 17: r16: Final 2D track with EO and P-RF fusion, passive RF location estimates are used until the EO only forms a consistent track for each drone, device ID is associated via RF fingerprinting

are EO detections available before passive RF detections (due to offsets of the two types of sensors and/or when drones are silent), tracks are labeled only with a notional ID obtained via the Hungarian data association with EO.

Analyzing r16—In r16, IF1200 and m600 fly simultaneously. These two drones are relatively larger and heavier than the ones in r14. Zoomed images from the EO sensor location are shown in Fig. 16.

While detailed figures are omitted for brevity, RPCA when optimized to detect objects with both positive and negative contrast with respect to the background is capable of detecting IF1200 and m600 few seconds after they appear in image data. Compared to Mavic and Phantom considered in r14, IF1200 and m600 are relatively large and have both negative and positive contrast compared to the image background, thus, fairly well detected in both versions of RPCA. DETR still finds it difficult to detect both IF1200 and m600 at the early stages.

In order to assign a label to each detected drone in the EO image plane, RF fingerprinting results are associated with EO detections. When tested with IF1200 (d101) and m600 (d104) in r16, Table 4 summarizes the average confidence over time which again shows the promise of proposed RF fingerprinting model for correct device identification.

Since the EO can detect the drones in r16 at very early stages using RPCA, passive RF based localization is used only until the device ID is associated with the EO detections for both drones. The combined tracker after running a Kalman filter on the 2D detections is shown Fig. 17.

Table 4: Average Confidence of Trained Deep Learning Model for RF Fingerprinting when Tested with IF1200 and m600 in r16p01

Tested Class	Avg Conf on IF 1200	Avg Conf on Mavic	Avg Conf on Phantom	Avg Conf on m600
IF1200	1	0	0.	0
m600	0	0	0.0002	0.9998

4. DISCUSSION

Based on the numerical studies done in this paper with the AFRL ESCAPE-2021 multi-modal dataset, we make several observations regarding detection, identification and tracking of Group 1 and 2 drones.

1. With only EO, Group 1 drones (DJI Phantom/Mavic) can be much better detected by advanced foreground/background separation algorithms compared to deep learning based techniques when the drones occupy only a small number of pixels in the image plane. RPCA can struggle detecting very small drones (e.g. Mavic in the very early portion of the trajectory) which can be compensated if passive RF is available
2. By incorporating device ID using passive RF, unique track ID could be obtained for the 2D track in the image plane. Thus, even when the passive RF is not available continuously, EO can still provide a device ID if EO can track the drone onwards
3. Group 2 (IF1200, m600) drones are quite reasonably well detected from the start of the trajectory (with the range considered in this paper) with EO only using RPCA. Still passive RF is useful to provide a unique track ID in the 2D image plane.

5. CONCLUSIONS

In this work, we quantified the detection, and tracking performance of small drones over range with EO using advanced foreground/background separation techniques (RPCA) as well as with combined EO and passive RF modalities. Compared to the most existing deep learning based solutions for drone detection and identification which perform poorly when the drones occupy only a small number of pixels of the image plane, to the best of author’s knowledge, this is the first paper to quantify the range sensitivity for small drone (Group 1, 2) detection using EO with foreground/background separation techniques. In order to label each detected drone in the image plane, the device ID obtained using passive RF fingerprinting is incorporated. For RF fingerprinting, a deep learning based model is trained to classify four drones in the AFRL ESCAPE 2021 dataset. After obtaining 3D locations with passive RF via TDOA based localization, and projecting the estimated locations to the image plane, track labels are assigned by detection-detection association. In the proposed architecture, it is sufficient to perform passive RF based localization until RPCA based EO detections pick the corresponding tracks. This is quite appealing since passive RF may not always be available in practical counter-UAS applications. In the future, we plan to perform Monte-Carlo analysis over a range of scenarios, runs, and passes to do track error analysis of the combined architecture with different types of drone trajectories (short, medium and long) to enhance our understanding of reliable drone detection with these two types of modalities. Future work also includes investigating incorporation of other modalities into the fusion framework such as acoustic and active radar and develop a

drone intent analysis algorithm using modal-specific features as well drone kinematics estimates.

6. APPENDIX

The augmented Lagrangian of (1), $F(L, S, E, Y)$, is given by,

$$\begin{aligned}
 F(L, S, E, Y) &= \|L\|_* + \tau\|S\|_1 + \lambda\|E\|_F^2 \\
 &+ \langle Y, X - L - S - E \rangle \\
 &+ \frac{\beta}{2}\|X - L - S - E\|_F^2
 \end{aligned}$$

where the matrix Y contains the Lagrange multipliers and $\beta > 0$. To find L, \hat{L} , keeping S and E fixed:

$$\begin{aligned}
 \hat{L} &= \arg \min_L \left\{ \|L\|_* + \frac{\beta}{2}\|X - L - S - E + \frac{1}{\beta}Y\|_F^2 \right\} \\
 &= \arg \min_L \left\{ \frac{1}{\beta}\|L\|_* + \frac{1}{2}\|L - (X - S - E + \frac{1}{\beta}Y)\|_F^2 \right\} \quad (3)
 \end{aligned}$$

The solution for (3) is given by [27]

$$\hat{L} = D_{\frac{1}{\beta}} \left(X - S - E - \frac{1}{\beta}Y \right)$$

where $D_\tau(Y) = UD_\tau(\Sigma)V^*$, is the singular value soft-thresholding operator where $D_\tau(\Sigma) = \text{diag}((\sigma_i - \tau)_+)$, $(x)_+ = \max(0, x)$, $Y = U\Sigma V^T$ is the SVD of Y of rank r with $\Sigma = \text{diag}(\sigma_{i_1 \leq i \leq r})$. To find S, \hat{S} , keeping L and E fixed,

$$\begin{aligned}
 \hat{S} &= \arg \min_S \left\{ \tau\|S\|_1 + \frac{\beta}{2}\|X - L - S - E\|_F^2 \right. \\
 &+ \left. \text{tr}(Y^T(X - L - S - E)) \right\} \\
 &= \arg \min_S \left\{ \frac{\tau}{\beta}\|S\|_1 + \frac{1}{2}\|S - (X - L - E + \frac{1}{\beta}Y)\|_F^2 \right\}
 \end{aligned}$$

for which the solution is given by soft-thresholding operator [27]:

$$\hat{S} = \Pi_{\frac{\tau}{\beta}} \left(X - L - E + \frac{1}{\beta}Y \right)$$

where $\Pi_\alpha(x) = \text{sign}(x).\max\{|x| - \alpha, 0\}$. To find E, \hat{E} , the following optimization problem is solved:

$$\begin{aligned}
 \hat{E} &= \arg \min_E \left\{ \lambda\|E\|_F^2 + \frac{\beta}{2}\|X - L - S + \frac{1}{\beta}Y\|_F^2 \right\} \\
 &= \arg \min_E \left\{ \frac{\lambda}{\beta}\|E\|_F^2 + \frac{1}{2}\|E - (X - L - S + \frac{1}{\beta}Y)\|_F^2 \right\}
 \end{aligned}$$

which reduces to

$$\hat{E} = \frac{1}{1 + 2\lambda/\beta} \left(X - L - E + \frac{1}{\beta} Y \right).$$

ACKNOWLEDGMENTS

This work was done under an independent research and development (IRAD) project funded by AMDS in JHU/APL. The data used in this work is part of ESCAPE 2021 data collect of Air Force Research Laboratory, AFRL/RI Rome, NY. Data was cleared for public release by AFRL, Case No: AFRL-2023-3379, on 17 July 2023. The authors would like to thank Dr Peter Zulch at AFRL/RI, Rome, NY for providing ESCAPE 2021 data and for insightful conversations on multi-modal data fusion.

REFERENCES

- [1] T. Humphreys, "Statement on the security threat posed by unmanned aerial systems and possible countermeasures," in *Overflight and Management Efficiency Subcommittee, Homeland Security Committee*, Washington, DC, US House, 2015.
- [2] A. Solodov, A. Williams, S. A. Hanaei, and B. Goddard, "Analyzing the threat of unmanned aerial vehicles (uav) to nuclear facilities," *Security J.*, vol. 31, no. 1, pp. 305–324, Feb. 2018.
- [3] A. Fotouhi, H. Qiang, M. Ding, M. Hassan, L. G. Giordano, A. Garcia-Rodriguez, and J. Yuan, "Survey on uav cellular communications: Practical aspects, standardization advancements, regulation, and security challenges," *IEEE Commun. Surveys Tuts.*, vol. 21, no. 4, pp. 3417–3442, 4th Quart. 2019.
- [4] K. Saylor, "A world of proliferated drones: A technology primer," in <https://www.cnas.org/publications/reports/a-world-of-proliferated-drones-a-technology-primer>, May 2018.
- [5] G. D. Cubber, "Explosive drones: How to deal with this new threat?" in *In Proceedings of the 9th International Workshop on Measurement, Prevention, Protection and Management of CBRN Risks*, International CBRNE Institute, Les Bons Villers, Belgium, 2019, pp. 1–8.
- [6] Online:, in <https://www.education.psu.edu/geog892/node/5>.
- [7] B. Taha and A. Shoufan, "Machine learning-based drone detection and classification: State-of-the-art in research," *IEEE Access*, vol. 7, pp. 138 669–138 682, 2019.
- [8] J. Wang and Y. L. H. Song, "Counter-unmanned aircraft system(s) (c-uas): State of the art, challenges, and future trends," *IEEE Aerosp. Electron. Syst. Mag.*, vol. 36, pp. 4–29, 2021.
- [9] B. K. Kim, H.-S. Kang, and S.-O. Park, "Drone classification using convolutional neural networks with merged doppler images," *IEEE Geosci. Remote Sens. Lett.*, vol. 14, no. 1, pp. 38–42, Jan. 2017.
- [10] M. Ezuma, F. Erden, C. K. Anjinappa, O. Ozdemir, and I. Guvenc, "Detection and classification of uavs using rf fingerprints in the presence of wifi and bluetooth interference," *IEEE Open Journal of the Communications Society*, pp. 60–76, 2019.
- [11] J. Barnard, "Small uav command, control and communication issues," in *Barnard Microsyst. Ltd.*, London, U.K., 2020.
- [12] P. Kosolyudhthasarn, V. Visoottiviseth, D. Fall, and S. Kashihara, "Drone detection and identification by using packet length signature," in *15th IEEE International Joint Conference on Computer Science and Software Engineering (JCSSE)*, July 2018, pp. 1–6.
- [13] V. Kartashov, V. O. I. Korytsev, S. Sheiko, O. Zubkov, S. Babkin, and I. Selieznov, "Use of acoustic signature for detection, recognition and direction finding of small unmanned aerial vehicles," in *15th IEEE International Conference on Advanced Trends in Radioelectronics, Telecommunications and Computer Engineering (TC-SET)*, 2020, pp. 1–4.
- [14] P. Zulch, "2021 escape ii data collection," *Air Force Research Laboratory (AFRL) RIGC, Internal Report, cleared for public release by AFRL, Case No: AFRL-2023-3379, on 17 July 2023*, Apr. 2023.
- [15] S. Singha and A. Burchan, "Automated drone detection using yolov4," in *Drones*, 2021.
- [16] O. Sahin and S. Ozer, "Yolodrone: Improved yolo architecture for object detection in drone images," in *44th IEEE International Conference on Telecommunications and Signal Processing (TSP)*, 2021, pp. 361–365.
- [17] A. K. M. Nalamati, N. M. Saqib, and M. Blumenstein, "Drone detection in long-range surveillance videos," in *In Proceedings of the 2019 16th IEEE International Conference on Advanced Video and Signal Based Surveillance (AVSS)*, Taiwan, China, Sept. 2019, pp. 18–21.
- [18] B. Taha and A. Shoufan, "Machine learning-based drone detection and classification: State-of-the-art in research," *IEEE Access*, vol. 7, no. 1, pp. 138 669–138 682, 2019.
- [19] S. Samaras, E. Diamantidou, D. Ataloglou, N. Sakellariou, A. Vafeiadis, V. M. A. Lalas, A. Dimou, D. Zarpalas, K. Votis, P. Daras, and D. Tzovaras, "Deep learning on multi sensor data for counter uav applications—a systematic review," *Sensors* 2019, 19, 4837. Available online: <https://www.mdpi.com/1424-8220/19/22/4837/dl40>, Apr. 2020.
- [20] F. Samadzadegan, F. D. Javan, F. A. Mahini, and M. Gholamshahi, "Detection and recognition of drones based on a deep convolutional neural network using visible imagery," in *Aerospace*, 2022.
- [21] N. Carion, F. Massa, G. Synnaeve, N. Usunier, A. Kirillov, and S. Zagoruyko, "End-to-end object detection with transformers," in *Retrieved from https://arxiv.org/abs/2005.12872*, 2020.
- [22] M. L. Pawelczyk and M. Wojtyra, "Real world object detection dataset for quadcopter unmanned aerial vehicle detection," *IEEE Access*, vol. 8, 2020.
- [23] P. Izmailov, D. Podoprikhin, T. Garipov, D. Vetrov, and A. G. Wilson, "Averaging weights leads to wider optima and better generalization," in <https://arxiv.org/abs/1803.05407>, 2018.
- [24] M. Piccardi, "Background subtraction techniques: a review," in *IEEE International Conference on Systems, Man and Cybernetics (IEEE Cat. No. 04CH37583)*, vol. 4, 2004, p. 3099–3104.
- [25] J. S. Kulchandani and K. J. Dangarwala, "Moving object detection: Review of recent research trends," in

IEEE International Conference on Pervasive Computing, 2015.

- [26] C. Guyon, T. Bouwmans, and E. Zahzah, “Robust principal component analysis for background subtraction: Systematic evaluation and comparative analysis,” in *Principal Component Analysis*, P. Sanguansat, Ed., chapter 12. InTech, 2012, 2012.
- [27] O. Oreifej, X. Li, and M. Shah, “Simultaneous video stabilization and moving object detection in turbulence,” *IEEE T-PAMI*, vol. 35, no. 2, p. 450–462, 2013.
- [28] E. J. Candès, X. Li, Y. Ma, and J. Wright, “Robust principal component analysis?” *J. ACM*, vol. 58, no. 3, pp. 1–37, 2011.
- [29] H. C. Schau and A. Z. Robinson, “Passive source localization employing intersecting spherical surfaces from time-of-arrival differences,” *IEEE Trans. Acoust. Speech*, vol. 35, p. 1223–1225, 1987.
- [30] R. Burkard, M. Dell’Amico, and S. Martello, *Assignment Problems*. Society for Industrial and Applied Mathematics, Philadelphia, PA, 2009, 2009.

the Engagement Optimization Group in the Air and Missile Defense Sector.



Tony Davis is a technical staff employee of the Air and Missile Defense sector of Johns Hopkins University Applied Physics Lab. He has a Master’s degree in artificial intelligence from Florida Atlantic University and has published research on optimizing drone flight planning with AI. His professional background includes machine learning software development for drug discovery at

Deep Forest Sciences, mechanical engineering at Motorola Solutions, and the US Army.

BIOGRAPHY



Thakshila Wimalajeewa Wewelwala (S’07, M’10, SM’18) received her B.Sc. degree in electronic and telecommunication engineering from the University of Moratuwa, Sri Lanka, in 2004, and the M.S. and Ph.D. degrees in electrical and computer engineering from the University of New Mexico, Albuquerque, NM, USA, in 2007 and 2009, respectively.

She was with the Department of Electrical Engineering and Computer Science, Syracuse University, Syracuse, NY, as a post doctoral research scholar from 2010 to 2012, and research faculty from 2012 to 2018. After working for BAE Systems as a Principal Research Scientist from 2018 to 2021, she joined the Johns Hopkins University Applied Physics Laboratory in 2021 as a Senior Professional Staff member. She is a Senior Member of IEEE and the Senior Editor of the Networked Sensor Systems area of IEEE Transactions on Aerospace and Electronic Systems. She is a recipient of the Jean-Pierre Le Cadre Paper Award at the 21st International Conference on Information Fusion in 2018. Her research interests span areas of statistical signal processing, multi-sensor/multi-modal data fusion and deep learning.



Thomas W. Tedesso received the B.S. degree from the Illinois Institute of Technology, Chicago, IL, USA, in 1990, the M.S. and Ph.D. degrees from the Naval Postgraduate School, Monterey, CA, USA, in 1998 and 2013, respectively, all in electrical engineering. He served in various assignments both ashore and afloat as a surface warfare officer trained in naval nuclear propulsion

and as an Assistant Professor with the United States Naval Academy, Annapolis, MD, USA. He retired from the United States Navy in November 2018. He joined the Johns Hopkins University Applied Physics Laboratory as a Senior Professional Staff member in September 2018 and is currently serving in the role of the Assistant Group Supervisor of